Available online at www.sciencedirect.com
ScienceDirect
Journal of Catalysis 251 (2007) 145–152
JOURNAL OF CATALYSIS
www.elsevier.com/locate/jcat

Sulfonic acid-functionalized silica-coated magnetic nanoparticle catalysts

Christopher S. Gill, Bryant A. Price, Christopher W. Jones *

School of Chemical & Biomolecular Engineering, Georgia Institute of Technology, 311 Ferst Dr., Atlanta, GA 30332-0100, USA

Received 29 March 2007; revised 3 July 2007; accepted 7 July 2007

Available online 23 August 2007

Abstract

Four different sulfonic acids are grafted onto silica-coated magnetic nanoparticle supports, yielding magnetic, solid acid catalysts. The hybrid organic/inorganic sulfonic acid catalysts are evaluated in test reactions in terms of activity and recyclability and compared with commercially available heterogeneous acidic resins and homogeneous sulfonic acids. The magnetic, solid acid catalysts exhibit comparable activity to the other commercial and homogeneous catalysts. Recovery tests confirm the presence of surface-bound sulfonic acid functionalities in three of the four catalysts. These results illustrate the utility of magnetic nanoparticles as a heterogeneous support for the simple recovery of sulfonic acid catalysts.

Keywords: Solid acid catalyst; Nanoparticle; Silica-coated nanoparticle; Supported sulfonic acid; Organic/inorganic hybrid catalyst

1. Introduction

The facile recovery and reuse of homogeneous catalysts via covalent tethering to a heterogeneous support while maintaining high catalytic activity has long been a goal in catalysis research [1]. These hybrid organic/inorganic catalysts have used various support materials, including porous inorganic oxides, such as zeolites, MCM, and SBA-type silicas, because of their high surface areas and well-defined structures [2–5]. In addition, organic polymers have also been extensively investigated as catalyst supports [6,7]. However, these materials can suffer decreased catalytic activity resulting from diffusion limitations as chemicals diffuse through the porous silica networks or through swollen polymeric resins. Consequently, recoverable soluble catalysts have received increasing attention in recent years. Methods for the recovery of soluble catalysts include soluble polymer, multiphase, and membrane systems [8]. In the case of soluble polymer and multiphase systems, the addition of solvent to selectively precipitate polymer or extract homogeneous catalysts can prove costly.

Nanoparticles have received increasing attention as an alternative support for catalysis. As the diameter of the particle decreases to the nanometer scale, ample external surface area becomes available for surface modifications. In addition, these particles can be dispersed into solvents, forming stable dispersions. However, these nanoparticles can be difficult to recover, as is the case with nonmagnetic nanoparticle-supported catalysts. Catalysts supported on magnetic nanoparticles (MNPs), usually iron oxides, can be quickly and easily recovered in the presence of external magnetic fields for reuse. In addition, internal diffusion limitations can be avoided, because all of the available surface area of the nonporous MNP is external. The surface of the MNPs can be functionalized to accommodate a wide variety of organic and organometallic catalysts. The various types of transition metal-catalyzed reactions using catalytic sites grafted on MNPs that have emerged recently include carbon–carbon cross-coupling reactions [9–14], hydroformylation [15,16], hydrogenation [17–19], and polymerization [20] reactions. Other reports of MNP-supported catalysts include enzymes for carboxylate resolution [21], amino acids for ester hydrolysis [22], and organic amine catalysts promoting Knoevenagel and related reactions [23,24]. Despite the occurrence of these MNP-supported base catalysts in the literature, no reports of acid-functionalized MNP catalysts are known to us.

Acid catalysts are used in a variety of industrial organic transformations, including aldol condensations, hydrolyses, acylations, nucleophilic additions, and others [25]. However, waste neutralization, difficult separations, reactor corrosion, and the inability for reuse have hindered industrial reactions

* Corresponding author. Fax: +1 404 894 2866.
E-mail address: cjones@chbe.gatech.edu (C.W. Jones).

0021-9517/$ – see front matter
doi:10.1016/j.jcat.2007.07.007

when using soluble, liquid acids [25]. Consequently, the need for solid acid catalysts has arisen. Proton-exchanged aluminosilicate zeolites are well suited to the petrochemical industry due to their high selectivity and ability to be used in continuous processes [26]. However, the small pore diameter of these acidic aluminosilicate zeolites limits their utility in processes in which larger molecules cannot penetrate to the interior of the catalyst. Inorganic supports of larger pore diameters were developed to address such problems. Acid sites in aluminosilicate derivatives of MCM-41 and SBA-15 materials were found to be only mildly acidic [27], and researchers began experimenting with covalently grafting sulfonic acids to these mesoporous supports to generate strong acid sites on these materials. These methods include oxidation of immobilized thiols to a sulfonic acids [28], hydrolysis of immobilized sulfonic acid chlorides [29], sulfonation of supported phenyl groups [30], ring opening of perfluorosulfonic acid sultones [31,32], and immobilization of perfluorosulfonic acid triethoxysilanes [33]. These methods and others have been thoroughly discussed in two reviews [25,27].

The present contribution builds on previous work with magnetic nanoparticle base catalysts [23,24] and illustrates for the first time the immobilization of sulfonic acid groups on magnetic nanoparticles for use as recyclable, solid acid catalysts. Various sulfonic acids were synthesized to compare the relative catalytic activity and stability of each. The magnetic nanoparticle supports were synthesized using known methods and then coated with silica, providing an inert barrier between the metal oxide core and surface functional groups. The hybrid organic/inorganic, magnetic, solid acid catalysts were characterized via nitrogen physisorption, FTIR, titration, XRD, and TEM. The active solid acid catalysts were easily recovered in the presence of an external magnetic field and exhibited good recyclability. Sulfonic acid catalysts grafted on mesoporous SBA-15 were observed to exhibit higher activities than those grafted on the silica-coated magnetic nanoparticles.

2. Experimental

2.1. Chemicals and instrumentation

Ammonium hydroxide (Fisher, 29%, v/v, aqueous solution), benzaldehyde dimethylacetal (Acros, 99%), cobalt(II) chloride (Alfa Aesar, anhydrous, 99.5%), chloroform (Sigma-Aldrich, anhydrous, 99%), dichloromethane (DCM) (Sigma-Aldrich, 99.8%), diethylamine (Acros, 99%), dimethylsulfoxide (DMSO) (Alfa Aesar, anhydrous, 99.8%), dodecane (Acros, 99%), ethanol (J.T. Baker, anhydrous, 94.7%), hydrochloric acid (J.T. Baker, 37%), hydrogen peroxide (EMD, 30%, v/v, aqueous solution), iron(II) chloride (Alfa Aesar, anhydrous, 99.5%), methylamine (Alfa Aesar, 40%, w/w, aqueous solution), nitric acid (Sigma-Aldrich, 70%), Pluronic 123 (Aldrich), sodium dodecylsulfate (SDS) (Acros, 85%), sulfuric acid (J.T. Baker, 96.4%), tetraethylorthosilicate (TEOS) (Acros, 98%), tetrahydrofuran (THF) (Sigma-Aldrich, 99%), *p*-toluenesulfonic acid monohydrate (Aldrich, 98.5%) and triethylamine (Alfa Aesar, 99%) were used as received. Toluene (J.T. Baker, anhydrous, 99.5%) was dried and deoxygenated with a solvent purification system [34] and stored in a nitrogen glove box. Silanes 3-mercaptopropyltrimethoxysilane (MPTMS) (Alfa Aesar, 97%) and chlorosulfonylphenyltrimethoxysilane (CSPTMS) (Gelest, 50% in dichloromethane) were stored in a nitrogen glove box. Hexafluoro(3-methyl-1,2-oxathietane)-2,2-dioxide (FSAS) (Synquest Labs, 95%) was stored at −35 °C under dry nitrogen. Triethoxysilylperfluorosulfonyl fluoride $(EtO)_3Si(CH_2)_3(CF_2)_2O(CF_2)_2SO_2F$ (FS-FTES) was obtained as a gift from DuPont and stored at 0 °C. Standard Schlenk techniques and an MBraun UniLab 2000 drybox were used as noted.

A Sonics VCX 750 ultrasonic processor was used for sonication during the silica-coating process. A Fischer Scientific FS60H sonication bath was used for all other sonication purposes. X-ray diffraction (XRD) spectra were obtained using a Scintag X1 powder diffractometer equipped with a Cu$K\alpha$ source. Nitrogen physisorption experiments were conducted using a Micromeritics ASAP 2010 system. Samples were dried under vacuum at 150 °C overnight before testing. Surface areas were calculated using the BET method. Transmission electron microscopy (TEM) studies were performed using a Hitachi HD-2000 field emission gun microscope. Fourier transform infrared (FTIR) experiments were conducted on a Bruker IFS 66v/s spectrometer. Samples were dispersed in potassium bromide pellets for analysis. Reaction conversions were monitored based on gas chromatography (GC) analyses in reference to a dodecane internal standard using a Shimadzu GC-2010 instrument furnished with a flame ionization detector (FID) and an SHRX5 column (15 m long, 0.25 mm i.d., 0.25 μm film thickness). The oven was heated from 50 to 140 °C at a rate of 30 °C/min and from 140 to 300 °C at a rate of 40 °C/min, and then held at 300 °C for an additional 2 min.

2.2. Preparation of silica-coated magnetic nanoparticles

Cobalt spinel ferrite ($CoFe_2O_4$) MNPs were synthesized as described previously [35]. The MNPs were washed three times with 100 mL of ethanol. The MNPs (about 1.7 g) were recovered magnetically and finally dispersed in 100 mL of ethanol, then coated with silica using a slightly modified procedure [15]. A solution of 11.76 mL of the ethanol–MNP dispersion (200 mg MNP) in 522 mL of isopropanol (IPA) and 40 mL of water was sonicated under mechanical stirring for 30 min. To this solution was added 46.6 mL of concentrated ammonium hydroxide, followed by the dropwise addition of a solution of 1 mL of tetraethylorthosilicate (TEOS) in 40 mL of IPA. The solution was mechanically stirred and sonicated for an additional 1 h. The silica-coated magnetic nanoparticles (SiMNPs) were recovered by centrifugation, washed three times with water, and then dried under vacuum at room temperature overnight.

2.3. Synthesis of SBA-15

SBA-15 [36] was synthesized following literature methods [37]. To a 1-L Erlenmeyer flask were added EO–PO–EO

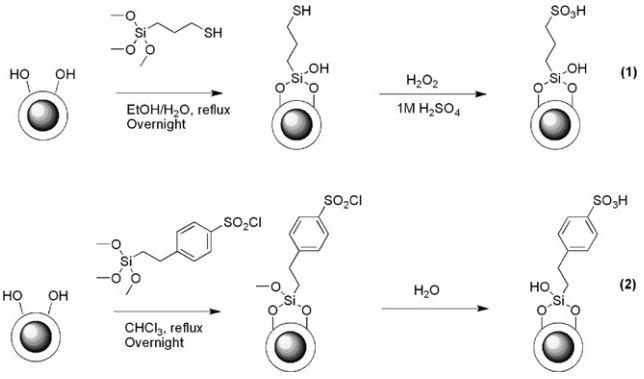

Scheme 1.

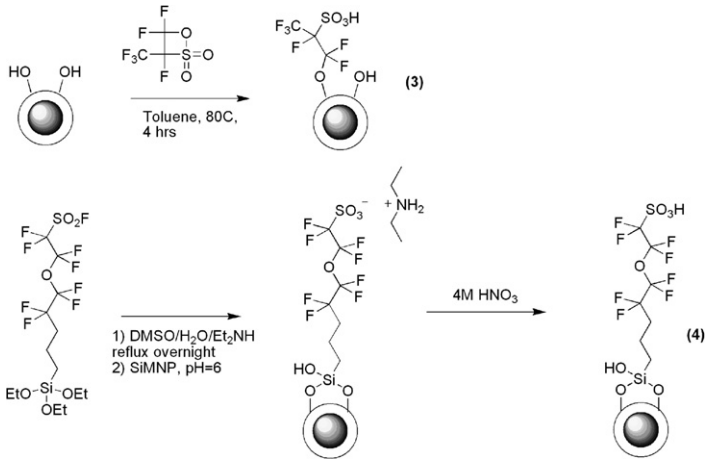

Scheme 2.

triblock copolymer (18.0 g), DI water (561 g), and concentrated HCl (99.5 g). This mixture was stirred overnight at room temperature to dissolve the polymer template. TEOS (39.8 g) was added to the solution and stirred for 5 min, followed by stirring at 35 °C for 20 h. A static treatment for 24 h at 80 °C was used to swell the pores. The mixture was decanted to remove most of the solution, and the white solid was filtered with 3 L of DI water, recovered, and dried at 60 °C for 24 h. The white powder was calcined to remove the polymer template using the following temperature profile: (1) heating to 200 °C at 1.2 °C/min, (2) holding at 200 °C for 1 h, (3) heating to 550 °C at 1.2 °C/min, (4) holding at 550 °C for 6 h, and (5) cooling to 200 °C at 1.2 °C/min.

2.4. Preparation of supported alkyl-sulfonic acid *1*

Supported sulfonic acid **1** was prepared (Scheme 1) via the oxidation of surface thiol functionalities [28]. To a solution of 1 g of MPTMS in 10 mL of ethanol and 10 mL of water was added 250 mg of SiMNP. The mixture was sonicated for 15 min and refluxed overnight. The SiMNP supported thiols (SiMNP–SH) were recovered magnetically and washed three times with 20 mL of water. The recovered SiMNP–SH was oxidized by reaction with 10 mL of 30% hydrogen peroxide in 10 mL of water and 10 mL of methanol overnight at room temperature. The product was recovered magnetically, washed three times with 20 mL of water, and reacidified with 10 mL of 1 M H_2SO_4. The sulfonic acid-modified SiMNPs (SiMNP–SO_3H) were washed three times with water and dried under vacuum at room temperature overnight.

2.5. Preparation of supported phenyl-sulfonic acid *2*

Supported phenyl sulfonic acid **2** was prepared (Scheme 1) via the hydrolysis of supported phenyl-sulfonic acid chlorides [29]. Using Schlenk techniques, 250 mg of SiMNPs were dried under vacuum at 150 °C overnight. In a nitrogen glove box, 1 g of CSPTMS 50% in DCM was diluted into 20 mL of chloroform. This solution was added to the SiMNPs and removed from the glove box. The mixture was sonicated for 15 min before refluxing overnight under an argon atmosphere. The phenyl-sulfonic acid chloride product (SiMNP–$PhSO_2Cl$) was exposed to the air, recovered magnetically, washed three times with 20 mL of DCM, and dried under vacuum at room temperature overnight. The SiMNP–$PhSO_2Cl$ was hydrolyzed to the phenyl-sulfonic acid product (SiMNP–$PhSO_3H$) by stirring in water overnight. The SiMNP–$PhSO_3H$ was washed three times with water and dried overnight under vacuum at room temperature.

2.6. Preparation of supported perfluoroalkylsulfonic acid *3*

Supported perfluoroalkylsulfonic acid **3** were prepared (Scheme 2) in a one-step reaction with 1,2,2-trifluoro-2-hydroxy-1-trifluoromethyl-ethane sulfonic acid beta-sultone (FSAS) [32]. Using Schlenk techniques, 250 mg of SiMNPs was dried under vacuum at 150 °C overnight. In a nitrogen glove box, 1 g of FSAS was diluted into 20 mL of anhydrous toluene. This solution was added to the SiMNP in a 125-mL screw-cap pressure reactor and removed from the glove box. The mixture was sonicated for 15 min before stirring at 100 °C for 4 h. The fluoro-sulfonic acid product (SiMNP–FSO_3H) was washed three times with 20 mL of anhydrous toluene and dried under vacuum at room temperature overnight.

2.7. Preparation of supported perfluorosulfonic acid *4*

Supported perfluorosulfonic acid **4** was prepared (Scheme 2) according to slightly modified procedures [33]. A mixture of 2.32 mL of water, 1.2 mL of DMSO, 0.48 mL of diethylamine, and 250 mg of triethoxysilylperfluorosulfonyl fluoride (FS-FTES) was refluxed overnight. SiMNPs (300 mg) were added to this solution, which was then sonicated for 30 min. The solution was neutralized with the dropwise addition of 1 M HCl until a pH of 6 was reached. The dispersion was refluxed overnight. The recovered nanoparticles were washed three times with 20 mL of water and acidified by stirring in 20 mL of 4 M nitric acid overnight. The perfluorosulfonic acid-functionalized SiMNPs (SiMNP–$SiFSO_3H$) were washed three times with 20 mL of water and dried overnight under vacuum at 80 °C.

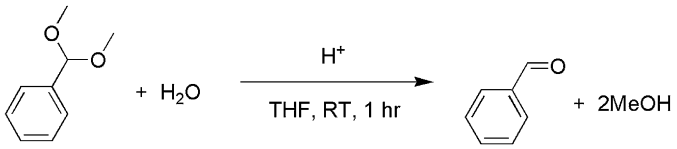

Scheme 3.

2.8. Solid acid titrations

Titrations were used to determine the acid loading of the catalysts. The surface-bound acidic protons were ion-exchanged with a brine solution by sonicating the SiMNP catalyst (50 mg) in saturated aqueous NaCl solution (10 mL). The SiMNP catalyst was recovered magnetically, and the brine solution was decanted and saved. This process was repeated twice more, yielding 30 mL of proton-exchanged brine solution. Two drops of phenol red indicator solution (2 mg in 10 mL of water) were added to the brine solution. The solution was titrated to neutrality using 0.1 M NaOH solution to determine the loading of acid sites on the SiMNP catalysts.

2.9. Acid-catalyzed reactions

The four solid acid catalysts were evaluated in the deprotection reaction of benzaldehyde dimethylacetal (Scheme 3). Into a 10-mL reactor was added 1 mol% SiMNP catalyst (0.004 mmol H^+) and 2 mL tetrahydrofuran (THF). This mixture was sonicated for 10 min to disperse the catalyst. The reaction was initiated by the addition of a solution of benzaldehyde dimethylacetal (BADMA) (60 μL, 0.4 mmol), THF (2 mL), dodecane (45.5 μL, 0.2 mmol), and water (7.2 μL, 0.4 mmol). Reaction conversion was monitored by GC in reference to the dodecane internal standard.[1] Catalysts **1**–**4** were compared against several homogeneous and heterogeneous sulfonic acid catalysts, including methanesulfonic acid, *p*-toluenesulfonic acid, triflic acid, Amberlyst A-15 resin, and Nafion powder.[2] Catalysts **1** and **4** also were prepared on mesoporous SBA-15 (designated **SBA1** and **SBA4**) to investigate the influence of the support on catalyst activity.[3]

Control reactions were performed to confirm that sulfonic acid sites were the catalytically active species. Controls were performed on the bare supports: MNP, SiMNP, and SBA-15. Additional controls were performed on intermediates in the syntheses of the catalysts **SBA1** and **SBA4** (Schemes 1 and 2). A final control was carried out on SiMNP treated with 4 M HNO_3 to determine whether the washing steps in the synthesis of **4** were sufficient to remove all homogeneous acid from the support.

[1] In cases requiring less than 5 mg SiMNP catalyst, a tenfold mass of catalyst was thoroughly dispersed into a THF solution and fractionated to yield the correct mass of catalyst. The volume of THF solvent added to the reaction was adjusted accordingly to total 4 mL.

[2] Loadings for Amberlyst A-15 and Nafion were obtained from manufacturers' literature.

[3] In cases requiring less than 5 mg of SBA catalyst, the reaction was scaled up to utilize >10 mg to minimize error when measuring catalyst masses.

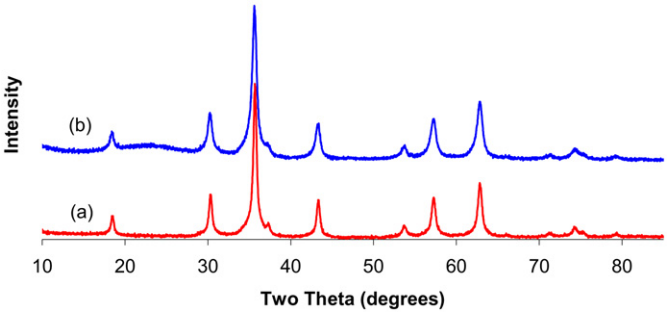

Fig. 1. XRD pattern of (a) bare MNP, (b) silica-coated MNP.

Recycling reactions were performed using the four SiMNP catalysts. On completion of the initial reaction, the catalyst was recovered magnetically, and the reaction solution was decanted. The catalyst was redispersed in THF (5 mL) by sonication for 10 min and recovered magnetically. This process was repeated twice more. After the third washing, the catalyst was dried under vacuum at room temperature. Recycle reactions were performed as described above.

Recovery tests were performed on the catalysts to evaluate whether the catalysis was occurring via surface-bound sulfonic acids. These reactions were prepared as specified above. However, the SiMNPs were recovered magnetically after a given time period (either 10 or 20 min), and the solution was decanted into a clean 10-mL reactor. The reaction solution was stirred and sampled for 60 min to elucidate whether conversion resulted from surface-bound acid sites or homogeneous acid leached from the support.

3. Results and discussion

3.1. Catalyst synthesis and characterization

Cobalt spinel ferrite MNPs were chosen as a catalyst support based on their high magnetic susceptibility [38] and ability for surface functionalization. These MNPs were coated with silica to provide an inert barrier between the reaction solution and the metal oxide core while maintaining the capacity for surface modifications and thermal stability. The silica coating was found to be necessary after failed attempts of immobilizing sulfonic acids via the oxidation of surface thiol groups using typical procedures [28]. The bare MNPs were found to be excellent catalysts for the rapid decomposition of hydrogen peroxide, preventing the thiols from being oxidized to the desired sulfonic acid. The incorporation of a silica shell was found to prevent peroxide decomposition and to maintain the ability for surface functionalization. The four immobilized sulfonic acids were chosen to illustrate a range in acidity from the less acidic alkyl-sulfonic acid to the perfluorinated superacids. The deprotection of benzaldehyde dimethylacetal was chosen as a simple benchmark reaction to evaluate the catalyst activity.

The solid acid catalysts were characterized using various methods. X-ray diffraction (XRD) of the bare MNP displayed patterns consistent with the patterns of spinel ferrites described in the literature (Fig. 1) [35]. The same peaks were observed

in the both the bare and silica-coated nanoparticle XRD patterns, indicating retention of the crystalline spinel ferrite core structure during the silica-coating process. The broad peak from $2\theta = 20°$ to 30° was consistent with an amorphous silica phase in the shell of the SiMNPs [39].

TEM images of the bare MNPs displayed aggregated nanoclusters, roughly 50 nm in diameter (Fig. 2). A close inspection of the images reveals that the clusters are formed of primary particles with diameters in the range of 6–8 nm. Images of the silica-coated magnetic nanoparticles display dark MNP cores surrounded by a lighter amorphous silica shell about 5–10 nm thick (Fig. 3). Instead of the desired core–shell architecture observed by others [15], the SiMNPs appeared to have been aggregated before silica coating.[4] Thus, they were coated as aggregates, leading to irregularly shaped particles ranging in size from 50 nm up to 1 μm.

Nitrogen physisorption experiments displayed a decrease in surface area on silica-coating of the MNPs. The bare MNPs and SiMNPs yielded BET surface areas of 126 and 48 m^2/g, respectively. The decrease in surface area resulted from aggregation of the particles before silica coating. Despite their nonuniform particle size and decreased surface area, the SiMNPs were suitable for surface functionalization and use as catalyst supports. Nitrogen physisorption experiments revealed a BET surface area of 837 m^2/g and an average pore diameter of 65 Å for the synthesized SBA-15 mesoporous silica.

Due to the paramagnetic nature of the nanoparticle core, nuclear magnetic resonance (NMR) techniques could not be used to confirm surface modifications on the SiMNPs. Instead, titrations and FTIR were used to characterize organic functionalities. Sulfonic acid loadings were calculated based on titrations of the proton-exchanged brine solutions. These data are summarized in Table 1. FTIR analysis of the SiMNPs showed similar spectra as seen in literature [40]. The O–H stretch and vibration of surface hydroxyl groups and physisorbed water were present as broad peaks at 3000–3700 cm^{-1} and a sharper peak at 1640 cm^{-1}, respectively. An intense peak at 1000–1250 cm^{-1} corresponded to the Si–O stretch in the amorphous silica shell. Evidence of the surface functionalization was difficult to observe due to the low loadings of catalysts **1**–**4**. The C–H stretch and C–H bend are visible in the spectra for catalysts **1**, **2**, and **4** at 2800–3000 cm^{-1} and 1400 cm^{-1}, respectively (Fig. 4). These peaks are absent from catalyst **3**, because no C–H bonds are present.

[4] The desired core–shell architecture was observed on smaller scale experiments. However, these results were difficult to replicate on the larger scale required for the chemical syntheses in this paper.

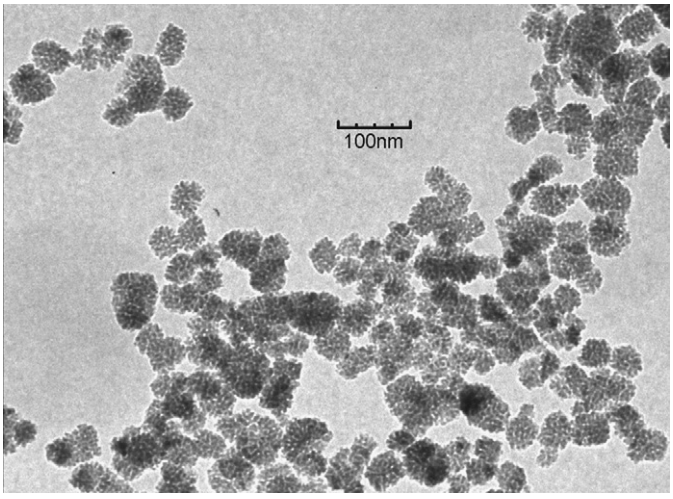

Fig. 2. TEM image of $CoFe_2O_4$ magnetic nanoparticles.

Table 1
Sulfonic acid loadings

Catalyst	Titration loading (mmol/g)
1, SiMNP–SO_3H	0.47
2, SiMNP–$PhSO_3H$	0.12
3, SiMNP–FSO_3H	0.78[a]
4, SiMNP–$SiFSO_3H$	0.055
SBA1, SBA–SO_3H	0.32
SBA4, SBA–$SiFSO_3H$	0.42

[a] Sulfonic acid loading for catalyst **3** calculated via thermogravimetric analysis due to leaching of the active acid.

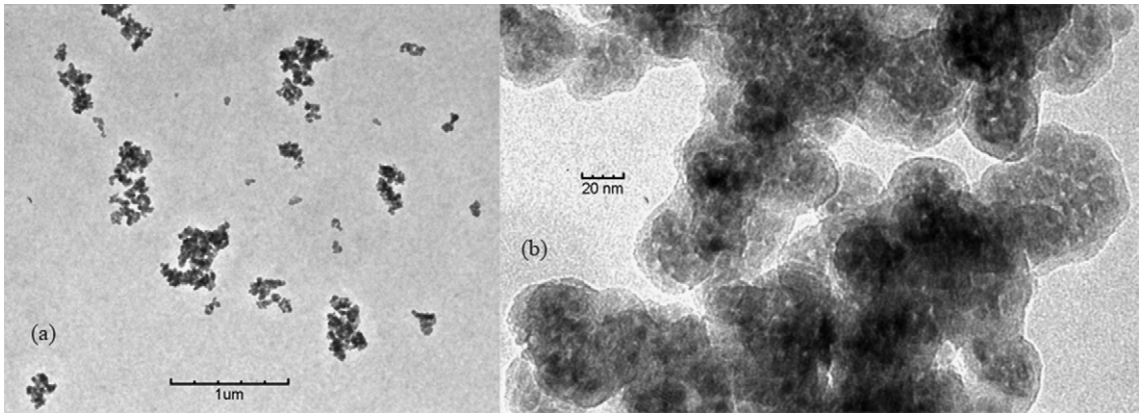

Fig. 3. TEM image of silica-coated $CoFe_2O_4$ magnetic nanoparticle supports at (a) 10,000 and (b) 200,000 magnification.

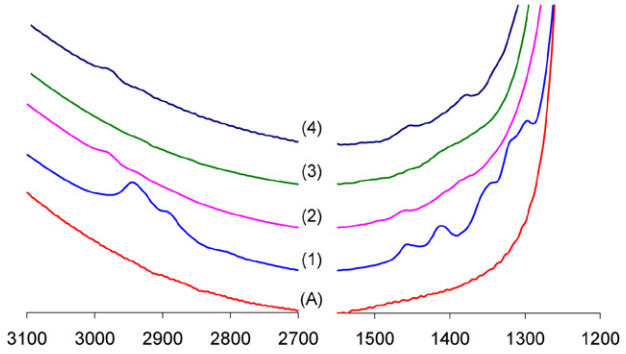

Fig. 4. FT-IR spectra of (A) non-functionalized SiMNP, SiMNP–SO_3H (1), SiMNP–$PhSO_3H$ (2), SiMNP–FSO_3H (3), SiMNP–$SiFSO_3H$ (4).

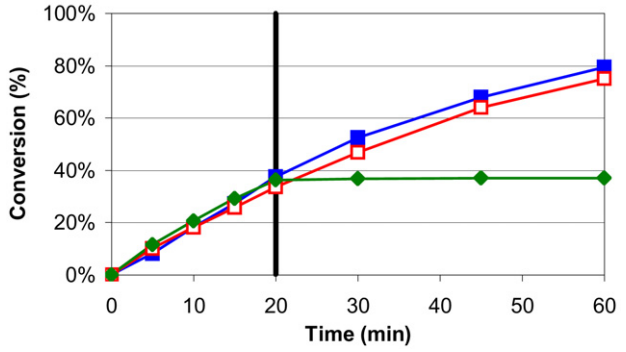

Fig. 5. Reaction conversion data for (1) SiMNP–SO_3H catalyst at 1 mol%: initial (■), recycle (□), and recovery test (◆).

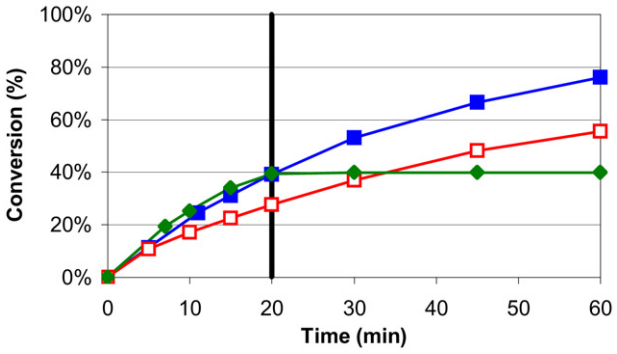

Fig. 6. Reaction conversion data for (2) SiMNP–$PhSO_3H$ catalyst at 1 mol%: initial (■), recycle (□), and recovery test (◆).

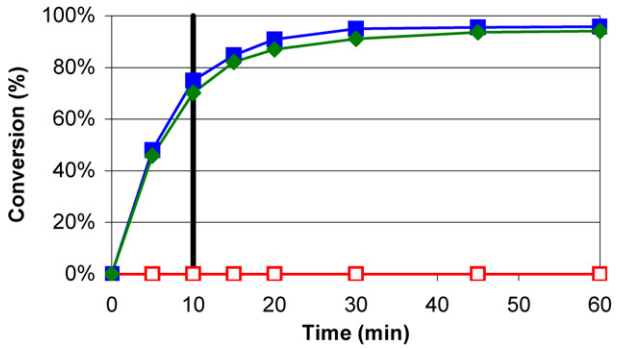

Fig. 7. Reaction conversion data for (3) SiMNP–FSO_3H catalyst: initial at 0.12 mol% (■), recycle (□), and recovery test (◆).

3.2. Catalytic studies

Kinetic profiles for the initial and recycle reactions of catalyst **1** closely overlapped each other within the limits of experimental error, reaching conversions of >75% in 60 min at 1 mol% catalyst (Fig. 5). The close overlap indicated that the catalyst was recyclable. The initial kinetic profile for catalyst **2** (Fig. 6) closely resembled that of catalyst **1**. However, the recycle reaction displayed a notable decrease in activity. A third recycle of this catalyst displayed no activity at all. In recovery tests, catalysts **1** and **2** were removed from the reaction media after 20 min, as indicated by the vertical line at 20 min in Figs. 5 and 6. The cessation of conversion after this time indicated that catalysis was occurring from surface-bound sulfonic acid sites. Control reactions on bare MNPs and bare SiMNPs displayed no activity after 60 min, indicating that neither the MNP core nor the silica-coated surface was responsible for the observed catalytic activity of catalysts **1–4**.

The initial kinetic profiles of catalysts **3** and **4** were markedly faster than those of **1** and **2** due to the strongly electronegative perfluoroalkyl linker adjacent to the sulfonic acid. Catalyst **3** reached 91% conversion in 20 min at 0.12 mol% catalyst (Fig. 7). However, a recycle reaction displayed no activity at all, suggesting that all active sulfonic acid species had been removed before running the recycle reaction. A recovery test for catalyst **3** at 0.12 mol% displayed no cessation of conversion on removal of the SiMNP support after 10 min. In addition, the kinetic profiles for the initial test and recovery test closely overlapped one another, indicating that catalyst **3** was not a heterogeneous catalyst, but simply a source of leached, catalytically active acid. The acid loss was presumed to occur via the reaction of water with the Si–O–C bond formed during the ring-opening reaction of the perfluorosulfonic acid sultone with surface silanol groups. The reaction was thought to hydrolize the Si–O–C bond, forming surface silanol groups and a leached perfluorosulfonic acid species, in accordance with literature reports [25]. Thus, when the SiMNP support was removed after 10 min, the leached active species continued catalyzing the reaction, leading to similar kinetics as observed in the initial reaction.

Conversion for **4** reached 96% in 5 min at 1 mol% and 72% in 20 min at 0.1 mol% catalyst. In contrast to the recovery test for **3**, the test for **4** showed a cessation of activity after 20 min, indicating a surface-bound active catalyst (Fig. 8). A recycle reaction of catalyst **4** showed similar activity as the initial reaction at 1 mol%, indicating that the catalyst was recyclable. A control reaction was performed to determine whether any physisorbed acid was responsible for the observed catalysis. Nonfunctionalized SiMNPs were treated with nitric acid, washed, and dried according to the synthetic procedure for catalyst **4**. This control reaction showed zero conversion after 60 min. These controls and kinetic data indicate that the catalytic activity resulted from surface-bound acid sites.

The alkylsulfonic acid and perfluoroalkylsulfonic acid catalysts **1** and **4** were prepared on mesoporous SBA-15 (**SBA1** and **SBA4**) to investigate any potential differences in catalytic

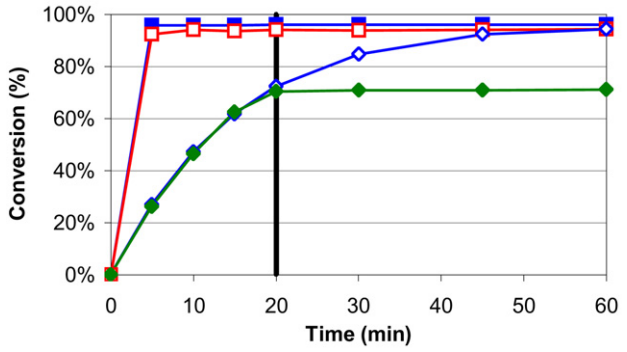

Fig. 8. Reaction conversion data for (4) SiMNP–$SiFSO_3H$ catalyst: initial at 1 mol% (■), recycle at 1 mol% (□), initial at 0.1 mol% (◇), and recovery test at 0.1 mol% (◆).

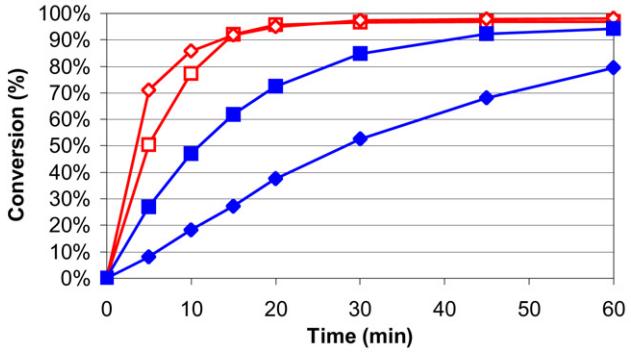

Fig. 9. Reaction conversion data for (**SBA4**) SBA–$SiFSO_3H$ at 0.1 mol% (□), (**SBA1**) SBA-SO_3H at 1 mol% (◇), (**4**) SiMNP–$SiFSO_3H$ at 0.1 mol% (■), and (**1**) SiMNP–SO_3H at 1 mol% (◆).

activity arising from the different supports. Kinetics were compared for the two catalysts at 1 mol% for **1** and **SBA1** and at 0.1 mol% for **4** and **SBA4** (Fig. 9). The concentration of perfluoroalkylsulfonic acid catalysts **4** and **SBA4** had to be compared at 0.1 mol%, because these catalysts reached 96 and 99% conversion in 5 min at 1 mol%, respectively. Conversion reached 96% for **SBA4** and 72% for **4** after 20 min at 0.1 mol%. A larger disparity in rates was observed for the alkylsulfonic acids **1** and **SBA1**. After 20 min, conversion reached 95% for **SBA1** but only 38% for **1** at 1 mol%. In both comparisons, the SBA-grafted catalysts exhibited faster rates than the SiMNP catalysts. A possible explanation for this may stem from enhanced physisorption of water in the SBA mesopores, resulting in higher local concentrations of water near the active sites. Diffusion limitations may slow kinetics for mesoporous silicas of smaller pore diameters [24]; however, the 65-Angstrom SBA-15 pores appeared to be sufficiently large to mitigate any diffusion effects in this case, because the SBA catalysts displayed faster kinetics than the nonporous SiMNP catalysts. Control reactions were performed on the intermediates in the syntheses of **SBA1** and **SBA4** to determine whether any unconverted, intermediary species were responsible for the activity in Fig. 9. SBA–SH and SBA–$SiFSO_3^-NH_2Et_2^+$ (intermediates of **SBA1** and **SBA4**) and nonfunctionalized SBA all displayed negligible conversion after 60 min, indicating that the sulfonic acid sites, not a precursor species, were responsible for the kinetic activity.

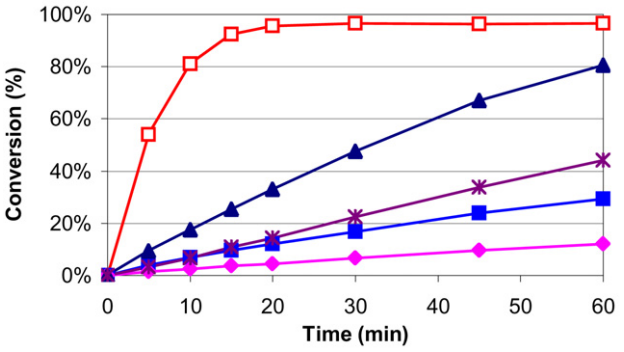

Fig. 10. Reaction conversion data for various sulfonic acid catalysts at 1 mol%: methanesulfonic acid (◆), *p*-toluenesulfonic acid (■), Amberlyst A-15 (*), Nafion powder (▲), and triflic acid at 0.1 mol% (□).

Table 2
Sulfonic acid catalyst initial turn over frequencies (TOF)

Catalyst	Homogeneous (min^{-1})	Heterogeneous (min^{-1})
Methanesulfonic acid	0.3	
Amberlyst A-15		0.8
p-Toluenesulfonic acid	0.8	
1, SiMNP–SO_3H		1.9
Nafion		1.9[a]
2, SiMNP–$PhSO_3H$		2.2
SBA1, SBA–SO_3H		14
3, SiMNP–FSO_3H		52[b]
4, SiMNP–$SiFSO_3H$		54
SBA4, SBA–$SiFSO_3H$		101
Triflic acid	108	

[a] TOF for Nafion was artificially low due to poor polymer swelling and inaccessibility of reactant to internal active sites.

[b] Catalyst **3** acted as a solid source of leached homogeneous acid.

Several commercially available sulfonic acids of varying strengths were tested at 1 mol% to compare to the synthesized catalysts (Fig. 10). The activity of the catalysts followed the order: methanesulfonic acid < *p*-toluenesulfonic acid (*p*-TSA) < Amberlyst A-15 < Nafion powder < triflic acid at 0.1 mol%. The trend followed the order of increasing electron-withdrawing capability of the functional groups adjacent to the sulfonic acid: alkylsulfonic acid < phenylsulfonic acid < perfluorosulfonic acid. The *p*-TSA and Amberlyst A-15 exhibited comparable kinetics for the first 15 min. After this time, the Amberlyst kinetics appeared marginally faster than for *p*-TSA. This was presumed to occur due to reactant absorption into the polystyrene beads of the Amberlyst, increasing the local concentration of reactant around the active sites and resulting in slightly faster kinetics. The macroreticular polymer resin appeared to swell sufficiently in the THF solvent to mitigate any diffusion limitations resulting in slowed kinetics. In contrast, the activity of Nafion powder was much lower than for its homogeneous comparison, triflic acid. This discrepancy in rates was attributed to diffusion limitations of reactant into the polytetrafluoroethylene (PTFE) support due to poor polymer swelling and inaccessibility of reactant to some internal, potentially catalytically active sites [41]. Differences in polymer swelling properties may explain the similar activities observed

for *p*-TSA and Amberlyst and the distinctly different rates seen for triflic acid and Nafion.

The maximum initial turnover frequencies (TOFs) for all catalysts investigated in this study are summarized in Table 2. Curiously, the TOFs for catalysts **1** and **2** were higher than those for their homogeneous comparisons, methanesulfonic acid and *p*-toluenesulfonic acid, respectively. Surface adsorption of reactants giving high local concentrations of reactant near the active sites could explain these enhanced rates. The opposite case was observed for the TOF of catalyst **4**, which was roughly half that of triflic acid. Catalyst **3** showed deceivingly high rates, although it must be considered a solid source of homogeneous catalyst, rather than a heterogeneous catalyst under the conditions investigated.

4. Conclusion

Hybrid organic/inorganic sulfonic acid/magnetic nanoparticle catalysts offer an alternative support to silica-based materials. Supporting these acid catalysts on silica-coated magnetic nanoparticles offers a simple and non-energy-intensive method for recovery and reuse of these catalysts. The silica coating provides an inert barrier to adverse interactions between surface functionalizations and the metal oxide core. The magnetic, solid acid catalysts exhibited comparable or better activities to other commercially available sulfonic acid catalysts, Amberlyst A-15 and Nafion. SiMNP catalysts **1**, **2**, and **4** were found to be easily recoverable, recyclable, and surface-bound solid acid catalysts. Catalyst **3** was observed to act as a source of homogeneous acid under these conditions, and may act as a recyclable, heterogeneous catalyst only under specific, anhydrous conditions. Catalyst **4** generated the highest TOFs of the magnetic solid acid catalysts, with an activity one half that of triflic acid. Catalysts **SBA1** and **SBA4** displayed enhanced activity when immobilized on 65-Angstrom mesoporous SBA-15 versus the nonporous SiMNPs. Further experimentation is needed to optimize the silica coating procedure on a large scale, to maximize the surface area available for surface chemistry.

Acknowledgments

This research was partially supported by the U.S. Department of Energy (CSG) and Air Products and Chemicals (B.A.P.—undergraduate research fellowship). The DOE-BES support is from Catalysis Science Grant DE-FG02-03ER15459. The authors thank Mark Harmer and DuPont for the gift of the perfluorinated silane. C.W.J. thanks the School of Chemical & Biomolecular Engineering at Georgia Tech for the J. Carl and Sheila Pirkle faculty fellowship.

References

[1] J.A. Gladysz, Chem. Rev. 102 (2002) 3215.
[2] D.E. De Vos, M. Dams, B.F. Sels, P.A. Jacobs, Chem. Rev. 102 (2002) 3615.
[3] A.P. Wight, M.E. Davis, Chem. Rev. 102 (2002) 3589.
[4] R. Anwander, Chem. Mater. 13 (2001) 4419.
[5] C.W. Jones, K. Tsuji, M.E. Davis, Nature 393 (1998) 52.
[6] N.E. Leadbeater, M. Marco, Chem. Rev. 102 (2002) 3217.
[7] B.M.L. Dioos, I.F.J. Vankelecom, P.A. Jacobs, Adv. Synth. Catal. 348 (2006) 1413.
[8] D.J. Cole-Hamilton, Science 299 (2003) 1702.
[9] Y. Zheng, P.D. Stevens, Y. Gao, J. Org. Chem. 71 (2006) 537.
[10] P.D. Stevens, G.F. Li, J.D. Fan, M. Yen, Y. Gao, Chem. Commun. (2005) 4435.
[11] P.D. Stevens, J.D. Fan, H.M.R. Gardimalla, M. Yen, Y. Gao, Org. Lett. 7 (2005) 2085.
[12] C. Duanmu, I. Saha, Y. Zheng, B.M. Goodson, Y. Gao, Chem. Mater. 18 (2006) 5973.
[13] Z.F. Wang, P.F. Xiao, B. Shen, N.Y. He, Colloids Surf. A Physicochem. Eng. Aspects 276 (2006) 116.
[14] Z.F. Wang, B. Shen, A.H. Zou, N.Y. He, Chem. Eng. J. 113 (2005) 27.
[15] R. Abu-Reziq, H. Alper, D.S. Wang, M.L. Post, J. Am. Chem. Soc. 128 (2006) 5279.
[16] T.J. Yoon, W. Lee, Y.S. Oh, J.K. Lee, New J. Chem. 27 (2003) 227.
[17] A.G. Hu, G.T. Yee, W.B. Lin, J. Am. Chem. Soc. 127 (2005) 12486.
[18] D.K. Yi, S.S. Lee, J.Y. Ying, Chem. Mater. 18 (2006) 2459.
[19] D. Guin, B. Baruwati, S.V. Manorama, Org. Lett. 9 (2007) 1419.
[20] S.J. Ding, Y.C. Xing, M. Radosz, Y.Q. Shen, Macromolecules 39 (2006) 6399.
[21] H.M.R. Gardimalla, D. Mandal, P.D. Stevens, M. Yen, Y. Gao, Chem. Commun. (2005) 4432.
[22] Y. Zheng, C. Duanmu, Y. Gao, Org. Lett. 8 (2006) 3215.
[23] N.T.S. Phan, C.S. Gill, J.V. Nguyen, Z.J. Zhang, C.W. Jones, Angew. Chem. Int. Ed. 45 (2006) 2209.
[24] N.T.S. Phan, C.W. Jones, J. Mol. Catal. A Chem. 253 (2006) 123.
[25] A. Corma, H. Garcia, Adv. Synth. Catal. 348 (2006) 1391.
[26] A. Corma, J. Catal. 216 (2003) 298.
[27] J.A. Melero, R. van Grieken, G. Morales, Chem. Rev. 106 (2006) 3790.
[28] W.M. Van Rhijn, D.E. De Vos, B.F. Sels, W.D. Bossaert, P.A. Jacobs, Chem. Commun. (1998) 317.
[29] J.A. Melero, G.D. Stucky, R. van Grieken, G. Morales, J. Mater. Chem. 12 (2002) 1664.
[30] C.W. Jones, K. Tsuji, M.E. Davis, Microporous Mesoporous Mater. 33 (1999) 223.
[31] M. Alvaro, A. Corma, D. Das, V. Fornes, H. Garcia, Chem. Commun. (2004) 956.
[32] M. Alvaro, A. Corma, D. Das, V. Fornes, H. Garcia, J. Catal. 231 (2005) 48.
[33] M.A. Harmer, Q. Sun, M.J. Michalczyk, Z.Y. Yang, Chem. Commun. (1997) 1803.
[34] A.B. Pangborn, M.A. Giardello, R.H. Grubbs, R.K. Rosen, F.J. Timmers, Organometallics 15 (1996) 1518.
[35] A.J. Rondinone, A.C.S. Samia, Z.J. Zhang, J. Phys. Chem. B 103 (1999) 6876.
[36] D.Y. Zhao, Q.S. Huo, J.L. Feng, B.F. Chmelka, G.D. Stucky, J. Am. Chem. Soc. 120 (1998) 6024.
[37] J.C. Hicks, C.W. Jones, Langmuir 22 (2006) 2676.
[38] Q. Song, Z.J. Zhang, J. Phys. Chem. B 110 (2006) 11205.
[39] P.S. Haddad, E.L. Duarte, M.S. Baptista, G.F. Goya, C.A.P. Leite, R. Itri, Prog. Colloid Polym. Sci. 128 (2004) 232.
[40] G.H. Du, Z.L. Liu, X. Xia, Q. Chu, S.M. Zhang, J. Sol–Gel Sci. Technol. 39 (2006) 285.
[41] M.A. Harmer, W.E. Farneth, Q. Sun, J. Am. Chem. Soc. 118 (1996) 7708.